https://doi.org/10.48048/tis.2023.6879

Identification Morphology and Magnetic Properties Sedimentary Elements Between Fossils and Outcrops Around the Lusi River: A Case Study of Central Java, Indonesia

Shandiyano Putra[1], Sumartina Gama Akmal[1], Budi Legowo[1], Budi Purnama[1,*], Agus Tri Hascaryo[2], Wahyu Widiyanta[3], Ilham Abdulah[3], Nur Kholish[3], Heru Dwiyantarai[3] and Hamdi Rifai[4]

[1]Department of Physics, Sebelas Maret University, Jawa Tengah 57126, Indonesia
[2]Departement of Environment, Faculty of Civil and Planning Technology, Islamic Indonesia University, Yogyakarta 55584, Indonesia
[3]Conservation Office of Sangiran Early Man Site, Sragen 57213, Indonesia
[4]Department of Physics, Universitas Negeri Padang, Padang 25131, Indonesia

([*]Corresponding author's e-mail: bpurnama@mipa.uns.ac.id)

Received: 19 March 2023, Revised: 12 April 2023, Accepted: 18 April 2023, Published: 28 August 2023

Abstract

Lusi River flows in the middle of Grobogan Regency with a length of 234 km and an area of 3,656.78 km^2. The warp river has many very diverse ends. One of them is the discovery of deer fossils estimated to be around 30,000 years ago and stored in the Pleistocene layer. There may be still many fossils stored in this layer that have never been studied. It is estimated that 80 % of fossils are incomplete because there are teeth attached to the fossils and the condition of the jaws is still neatly arranged. We get the magnetic susceptibility value around 1.3×10^{-8} - 37.8×10^{-8} m^3/kg. Vibrating Sample Magnetometer confirm that value of magnetic saturation about 0.071 - 0.176 emu/gr, magnetic remanent about 0.0001 - 0.004 emu/gr, and magnetic coercivity around 10.969 - 115.278 Oe. X-Ray Diffractometer confirm the mineral is Calcite ($CaCO_3$) and Quartz (SiO_2). From the results we got, it can be confirmed that the fossils found at the bottom of the Lusi river have the same minerals and elements as environmental sediments. So, fossils can be said to have been sedimented over a long period of time in the Lusi River.

Keywords: Lusi river, Sediment, Fossil, Morphology, Magnetic properties

Introduction

Indonesia is a vast country and known for its quaternary geology with discoveries of human and vertebrate fossils, especially in Sulawesi, Sumatera, Flores and Java. In Sulawesi, founded the paintings in the cave about 2.588 million years ago [1], and tools used by ancient people on the island of Sulawesi [2].The discovery of painting in a cave is also found at the Moon Hill, Sumatera [3]. Furthermore, the majority of discovery sites also found by archaeologists in Java, such as in Central Java [4,6]. Particularly in the Kendeng Zone and Solo Basin, such as the Ngandong [7], Sabungmacan [8], Trinil [9], and Sangiran [10], also in the southern part of Central Java, such as the Punung area **Figure 1**.

One of the famous prehistoric site is Sangiran which part of Kendeng Zone [11,12]. This site was designated a UNESCO World Heritage Site in 1996 with number 593 [13], due to fossil discoveries and the discovery of Homo erectus fossil approximate 1.5 million-year-ago (Ma), which complement world discoveries. High-resolution footage of the Matuyama-Brunhes transition showing the date of Javanese Homo erectus in the Sangiran dome [9]. Furthermore, in the northern part of Central Java, there are prehistoric sites such as the Patiayam area [14-16], near the foot of Mount Muria. In this site was founded stone artifacts and Homo erectus fossils as well as the discovery of 9 species of fossil fauna by Van Es that similar to Trinil fauna (Kendeng Zone) [17]. Physiography of Java Island, the Patiayam Hills are located in the north of the Central Java Coast, to the south of the Lusi River Valley, which also north of the Bengawan Solo River and Sangiran.

Because of the Lusi River spans 3 regions, it is possible that contains information about ancient life which connects discoveries in the northern and southern regions of Central Java. This is supported by the discovery of vertebrate bone fossil fragments around Lusi and the discovering human fossil fragments also ancient human tools, have thought lived during the Middle Pleistocene [18,19]. This indicated that Lusi River contains information about ancient life and have corelation between Sangiran-Bengawan Solo and

Patiayam. It is uncommon to come across archaeological researchers who are interested in paleomagnetism. Previous researchers investigated ancient life in terms of age, past life, culture, and items used.

We found a deer fossil in the Lusi River Basin that is in the form of a deer mandible. Because the jaw has teeth attached, the overall value is still around 70 - 80 %, and the jaw texture is still intact. In the fossil, there are rocks and mud that have undergone a sedimentation stage by river flow. There are fine scratches on the surface of the fossil that occurred due to the flow of the river at that time [20]. This flow resulted in an uneven distribution of rock patterns in the fossils. This is also evidenced by the presence of open outcrops. The outcrop contains soil of various characters. There are fine grains with a diameter between < 1 mm and rocks with a diameter of 1 - 6 mm, which are unevenly distributed at the outcrop's top, middle, and bottom outcrop shows the sedimentation process caused by the lusi river flow [21-23].

Unconfirmed outcrops are believed to contain minerals [24-26]. One of the methods that can be used is paleomagnetism. Paleomagnetism is the study of the recording of the Earth's magnetic field present in rocks, sediments, or archaeological materials [27,28]. Certain minerals in rock keep records of the direction and intensity of the magnetic field as it forms. These recordings provide information about the nature of the past. Much can be learned in the field of paleomagnetism one of them is mineralogy [29-31].

Mineralogy is a branch of geology that studies minerals, both individually and in a unitary form, including studying their physical properties, chemical properties, how they exist, how they occur, and how they are used. The mineral is a homogeneous solid object found in nature, formed inorganically, with a chemical composition within certain limits, and has atoms arranged in an orderly man. This study only focused on soil mineralogy.

Soil mineralogy is the study of solid minerals in the form of flat-boundary crystals [32,33]. Minerals have specific data field properties. The primary topic of discussion in soil mineralogy is rock. Meanwhile, soil organic matter, particularly soil or sediments found in fossils and outcrops, is not discussed in soil mineralogy. In this case, the researcher wants to look into the minerals in the 2 samples using the same method. The researchers analyzed whether or not the 2 samples contained the same minerals. If they are identical, the fossil is indeed from the study area. If it is not same, more research is needed to determine where the fossil came from. To determine whether the lower jaw fossils of deer were buried directly by the surrounding material or carried to the sampling area by the warp river's water flow. So, the purpose of this study is investigated of fossil we found it from mineral and magnetic compare with the outcrop on the surrounding environment.

Geological setting

Prehistoric sites in Java Island are close to another in Central Java. It was founded various types of fossils, with assumption the possibility for ancient human and fauna to travel or interact from the south (Sangiran) around Bengawan Solo River to the north (Patiayam) which around the Mount Muria in the Pleistocene, as shown in **Figure 1**. Several studies reveal how they interact and survive through rivers and hills.

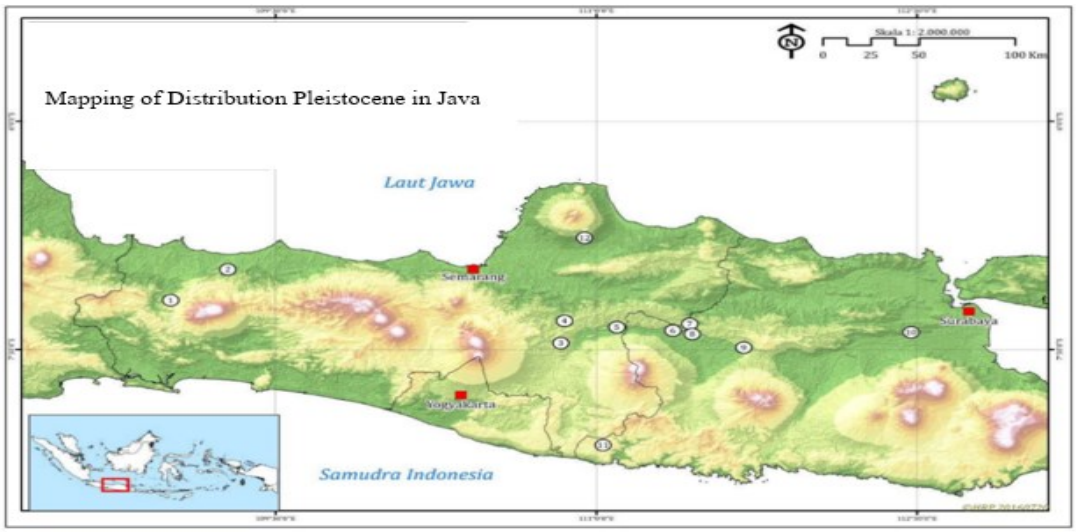

Figure 1 Prehistoric sites in Java on Pleistocene.

This study belongs to Lusi River as shown in **Figure 2** which includes the Wirosari sub-district, Grobogan district, Central Java. This river has a length of 234 km, with a width about 3,656.78 km^2. This river flows east to west between the Kudus, Pati and Rembang Hills to the north and the Kendeng Hills to the south [34,35]. The geographic area of the study area is shown in **Figure 2**-point C were, A: Muria Mountains Region; B: Demak Depression - Rembang Hills - Lasem Mountains; C: Lusi River Basin Region; D: Kendeng area in the south. The supply of eroded material from small rivers originating on the cliffs' slopes influences the sedimentation of the Lusi River.

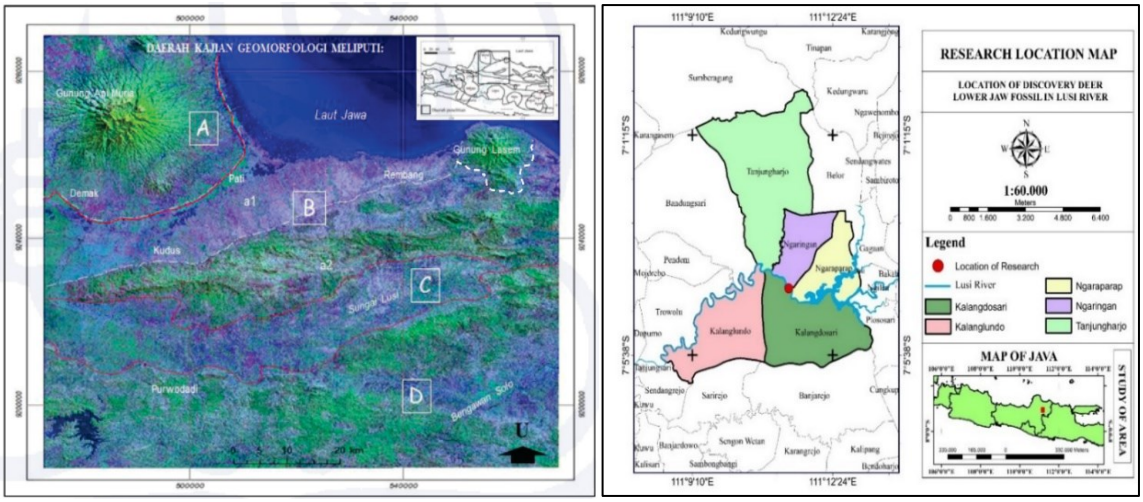

Figure 2 Geomorphology area of research location and this research belongs to the Ngaringan area.

We use sample fossil of a deer (*Cervidae*) and 3 sediments sample from outcrops around sampling area. This position was taken because there are outcrops that allow for sampling and are very far from residential areas. This river runs through rice fields and corn plantations owned by locals. They rarely use the river because of dirty water with a brown color makes residents unable to use the water for their daily needs. The river is divided into 2 sections: The side and the middle area. The side of the part of the river which has a distance of 5 - 10 m from the middle of the river is dominated by mud with a diameter of < 2 mm. The bottom of the river is dominated by blackish ash-colored mud and rocks that have quite a variety of diameters in the range of 1 - 3 mm which are spread unevenly. On the side of the river, some outcrops can be divided into 3 categories: The upper, middle, and lower parts see **Figure 3**.

The upper part is dominated by humus soil which is brownish black due to the presence of very dense smallholder plantations and surrounding trees with few rocks with a diameter of 1 - 5 mm. The black color is caused by the black soil color means that it includes fertile soil because it is rich in nutrients. Decaying organic matter or humus makes the soil darker in color. In the center, there is brownish red soil, and alluvial and still filled with rocks with a diameter of about 1 - 7 mm. The color is because it contains iron minerals and organic materials [36], which are included in the medium category. The bottom is dominated by mud and clay which is dominated by rocks with a diameter of 1 - 7 mm. The uneven distribution of rocks occurs because of the flow of the river which causes uneven rock transportation [37-39]. This uneven transportation causes the movement of material from one place to another.

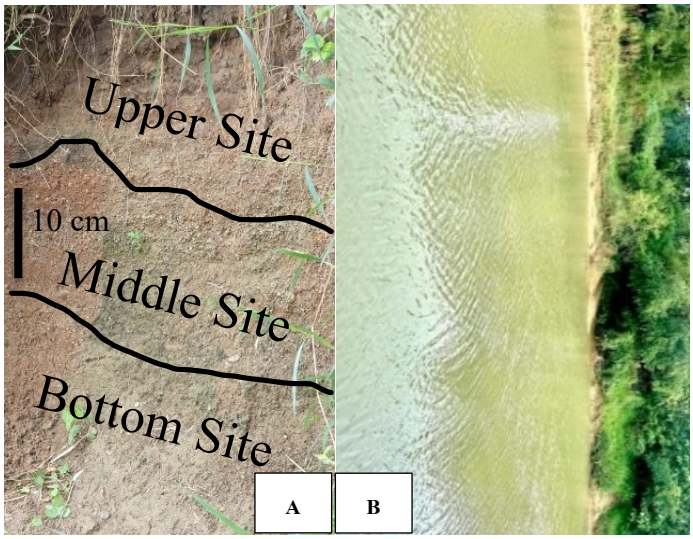

Figure 3 (A) The outcrops that include 3 various sediments and (B) One point in the Lusi River.

Several previously identified zones that have direct contact with warp sites are in the Sangiran area. In the Sangiran area, it then experienced a uniform shift towards the Patiayam site before heading to the Lusi archaeological site area. At the Sangiran site there are 4 formations that became the basis for ancient living things to reproduce. Then forwarded to the Patiayam site which has a correlation in the outcrops found. Because some of the outcrops were found to have a positive connection. However, the Lusi site has not found a positive correlation in the outcrops found to identify the distribution of ancient living things because we did not find another outcrop. However, during the field study conducted, several types of fossils were found that still had the same characteristics as the Sangiran and Patiayam sites.

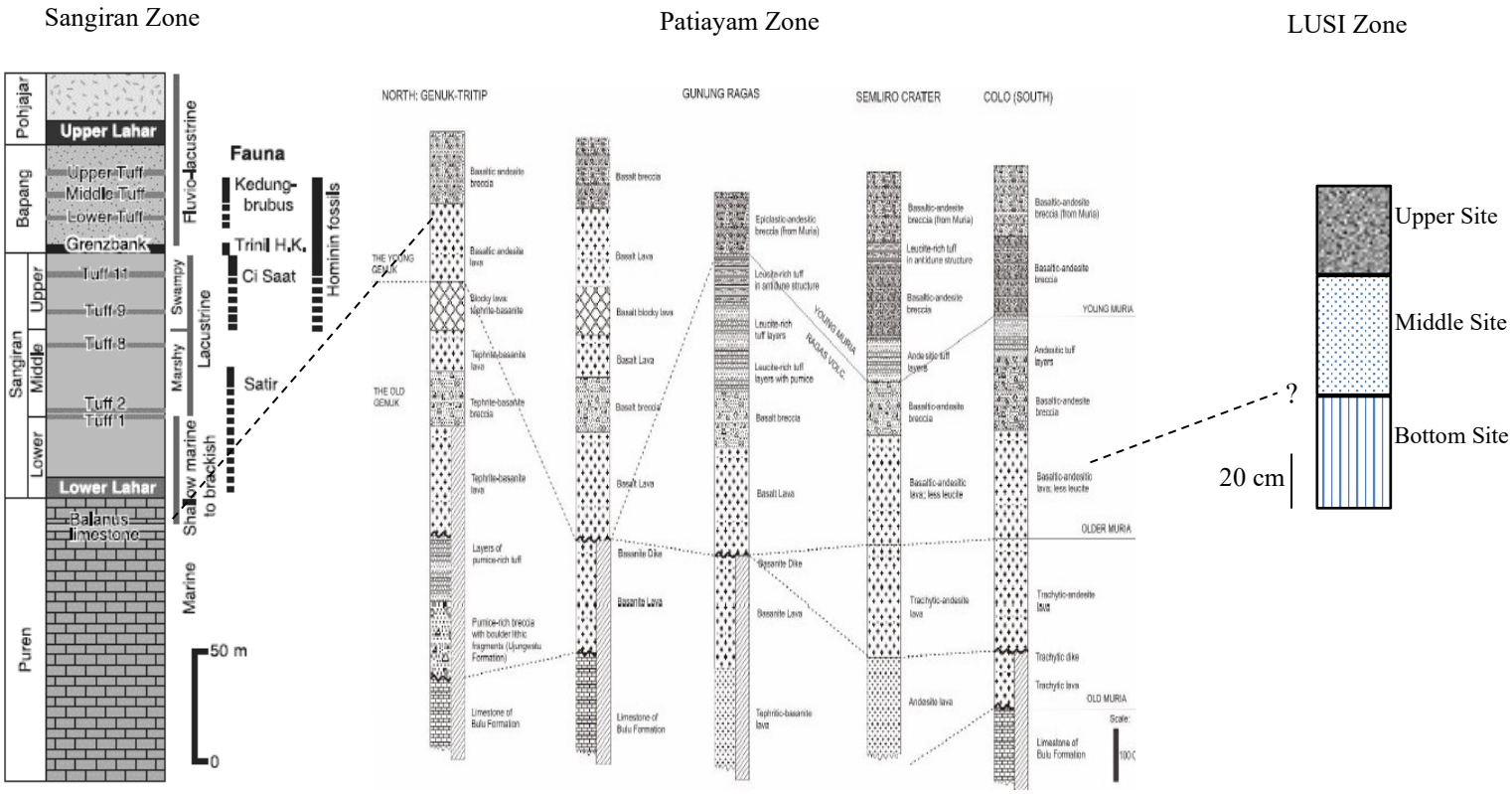

Figure 4 Some sites of stratigraphy zone in central java, a) Sangiran zone [10], b) Patiayam zone [40], and c) Lusi zone.

The upper part is dominated by humus soil which is brownish black due to the presence of very dense smallholder plantations and surrounding trees with few rocks with a diameter of 1 - 5 mm. The black color is caused by the black soil color means that it includes fertile soil because it is rich in nutrients. Decaying organic matter or humus makes the soil darker in color. In the center, there is brownish red soil, and alluvial and still filled with rocks with a diameter of about 1 - 7 mm. The color is because it contains iron minerals and organic materials which are included in the medium category. The bottom is dominated by mud and clay which is dominated by rocks with a diameter of 1 - 7 mm. The uneven distribution of rocks occurs because of the flow of the river which causes uneven rock transportation. This uneven transportation causes the movement of material from one place to another.

Materials and methods

In this study, we used 2 types of samples. First sample is fossil's sediments where deposition and hardening have occurred, and the second sample is pure sediments which still present in outcrops. The samples were brought to Sebelas Maret University to be prepared for various measurements. There are 8 samples in this study; 1 of sediment attached and hardened to fossils, 4 of fossil points obtained by fine drilling, and 3 pure sediments obtained from the outcrop where the fossils were discovered. Four points on the fossil samples have been obtained in powder form. so that only 4 sediment samples require further preparation. First step is the sediment samples washed using distilled water with a ratio of 1:1 [41-43]. After washing for 4 h using hot platted with 500 rpm [44,45], an interval of every 1 h the distilled water is replaced to clean the impurities attached to the sediment. After washing the samples were dried using a Memmert oven at 100 °C for 7 h to remove the moisture content in the samples.

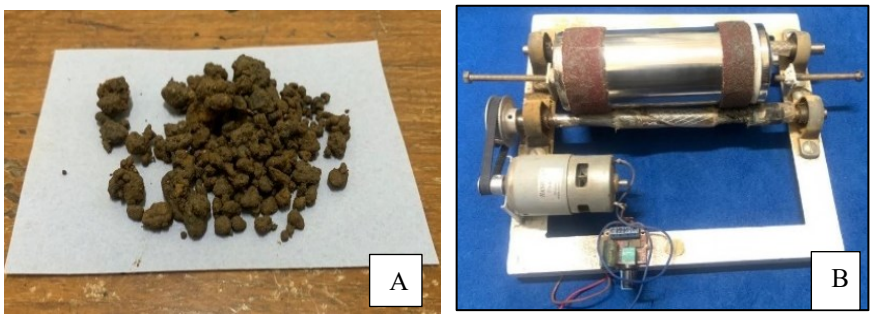

Figure 5 (A) The sediment sample with code BA in the outcrop (riverside) and (B) Ball milling tools to grind a sample for becomes very fine (powder).

Figure 5(A) show the sample ready to be crushed into macro by using a hammer aiming to break the rock contained in the sample into small rocks that can be forwarded to the next stage. It looks blackish brown because of contains water and consists of rocks with a diameter of 1 - 5 mm. After divided into small rocks, inserted into a tool called ball milling for the micro-refining process according to **Figure 5(B)** which aims to make the coarse grains into a very fine powder as shown at **Figure 6(A)**.

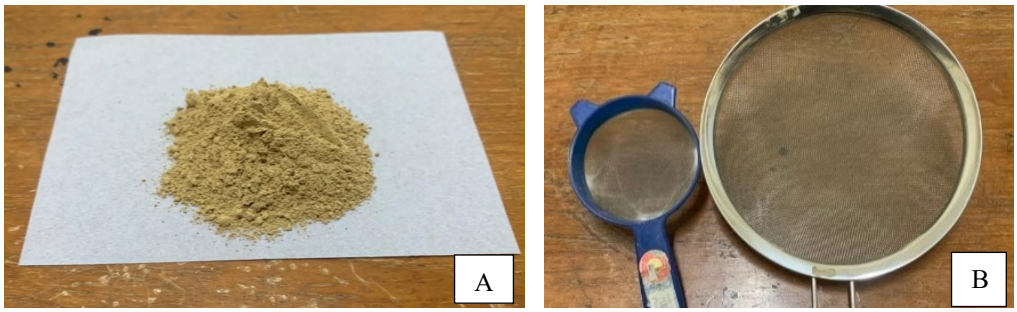

Figure 6 (A) Powder samples and (B) The sieve tools for granule separation process.

The powder sample were washed using hot plated 500 rpm distilled water in a ratio of 1:1 and heated using a Memmert oven at 100 °C and next carried out with filtering using tools in **Figure 6(B)**. After filtered, obtained the fine powder and the samples ready to be tested. To knowing magnetism susceptibility used Bartington MS2B magnetic susceptibility system. This tool works on 2 frequencies, 470 and 4,700 Hz at a magnetic field of 80 A/m rms also can measure the susceptibility from 0.001×10^{-6} m^3/Kg. Output of this measurements are mass-specific magnetic susceptibility at low frequency χ_{lf} was termed, mass-specific magnetic susceptibility at high frequency was termed χ_{hf} and frequency dependent magnetic susceptibility χ_{fd} was calculated.

$$\chi_{fd}\% = \frac{\chi_{lf}-\chi_{hf}}{\chi_{lf}} \times 100$$

Note: $\chi_{fd}\%$ is susceptibility frequency dependent, χ_{lf} is susceptibility low field (470 Hz) and χ_{hf} is susceptibility high field (4,700 Hz). Next measurement is X-Ray Diffractometer (XRD) to see the mineral contained, Vibrating Sample Magnetometer (VSM) to obtain the hysteresis parameters of saturated magnetization (Ms), remanent magnetization (Mr), coercivity field (Hc), also remanent coercivity field (Hr), and using Scanning Electron Macroscopic equipped with Energy Dispersive X-Ray Spectroscopy (SEM-EDS) to see the morphology and elements contained in the sample.

Table 1 Description of sample were taken in field.

Code	Coordinate	Description
AA	111° 11' 23.28"	The sample is fine gravel sand measuring about 1 - 2 mm
TA		Mixture samples of fine sand and rock. The sample size is about 2 - 6 mm.
BA		The type of sample that most often occurs in direct contact with the surface of the Lusi River when there is an increase in river water discharge.
SSFA	111° 12' 52. 42"	There is a process of sedimentation or direct contact with river water continuously. Thus, resulting in a pile of sediment that is on the surface of the fossil
T1		The first point when taking samples using a small scraper to get fossil powder before further testing.
T2		The second point before the next test is carried out
T3		The third point before testing
T4		The fourth point before testing. (All samples taken in the fossil from T1 - T4.

(a) (b) (c)

Figure 7 Appearance of animal fossils obtained during field studies; a) Complete fossil shape, b) The size of the fossil, and c) Point drilling is carried out to obtain fossil powder before further testing is carried out.

Results and discussion

Magnetic susceptibility (MS2B)

Table 2 show the result of magnetic susceptibility using Bartington MS2B. The measurement was carried out 3 times on each sample until obtained the average of each sample, the Low Field test (χlf) with range 16.2 - 1.2×10^{-8} m^3/Kg and (χhf) 15.6 – 1.2×10^{-8} m^3/Kg.

Table 2 Results of the mass-specific magnetic susceptibility measurements.

Categories	Code	Magnetic susceptibility ($\times10^{-8}$ m^3/Kg)								$\chi fd\%$
		Low field (χlf) 470 Hz			Avg	High field (χhf) 4,700 Hz			Avg	
Pure sediment	AA	15.9	16.7	16.7	16.2	15.1	15.9	15.9	15.6	3.3
	TA	22.9	20.9	22.2	22.4	20.9	20.9	20.9	20.9	6.8
	BA	16.1	16.1	16.1	16.1	16.1	16.1	16.1	16.1	0
Sediment on fossil	SSFA	37.8	37.8	37.8	37.8	37.8	37.8	37.8	37.8	0
Yellow river Sediment [46]		0.341 - 0.631								−0.204 - 0.865
Fossil powder	T1	1.5	1.2	1.1	1.3	1.5	1.2	1.2	1.3	0
	T2	1.4	1.3	1.2	1.2	1.4	1.1	1.2	1.2	0
	T3	1.5	1.2	1.1	1.3	1.4	1.2	1.3	1.3	0
	T4	1.3	1.2	1.2	1.2	1.3	1.2	1.2	1.2	0

From **Table 2** it is divided into 3 categories of different sample types. The 3 categories of samples contain various magnetic materials. Magnetic material appears due to interactions with the surrounding environment. The first category of susceptibility value is in the sediment in the outcrop due to direct contact with the environment and has a strong contribution to the contribution of magnetic material. Various values 15.9×10^{-8} - 22.9×10^{-8} m^3/Kg. The second category, namely sediments in fossils, has a high susceptibility value.

This is due to the occurrence of a continuous sedimentation process during the deposition process. Then the discovery of sediment that has been attached directly to the surface of the fossil. Then the last category is fossils. Magnetic susceptibility value 37.8×10^{-8} m^3/Kg. Compared with the magnetic susceptibility values obtained from Yellow River sediments, China. There are significantly different values. The content of magnetic elements in the Yellow River sediments is confirmed to be very low compared to the Lusi River sediments. So, the Lusi River contains a lot of magnetic elements, but is still classified as a low element content.

The third category is fossils. In this case what was found was a type of animal. The susceptibility values found in these fossils are categorized as weak or very small. Range between 1.3×10^{-8} - 1.5×10^{-8} m^3/Kg. Because the main constituents of fossils are Calcium and Carbon [47-49]. Calcium and Carbon are not included in the magnetic material, so that the measured susceptibility value is very small. Grouping of all samples is done using a scatter diagram **Figure 8**.

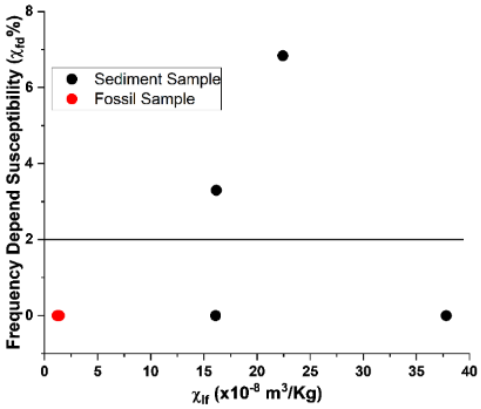

Figure 8 Scatter diagram between low field magnetic susceptibility (Xlf) and frequency dependent susceptibility (Xfd%). Three different groups were obtained.

In **Figure 8** it is clear the grouping of all samples. The samples with the fossil category are grouped into one. However, the categories of sediments and sediments attached to fossils are separated due to factors caused by the contribution of magnetic materials such as Fe.

X-ray diffractometer (XRD)

To see the minerals contained in the sample, testing was carried out using an X-Ray Diffractometer (XRD). The results obtained can be seen in **Figure 9**. We analyzed the minerals contained in the samples with the help of the RRUFF database.

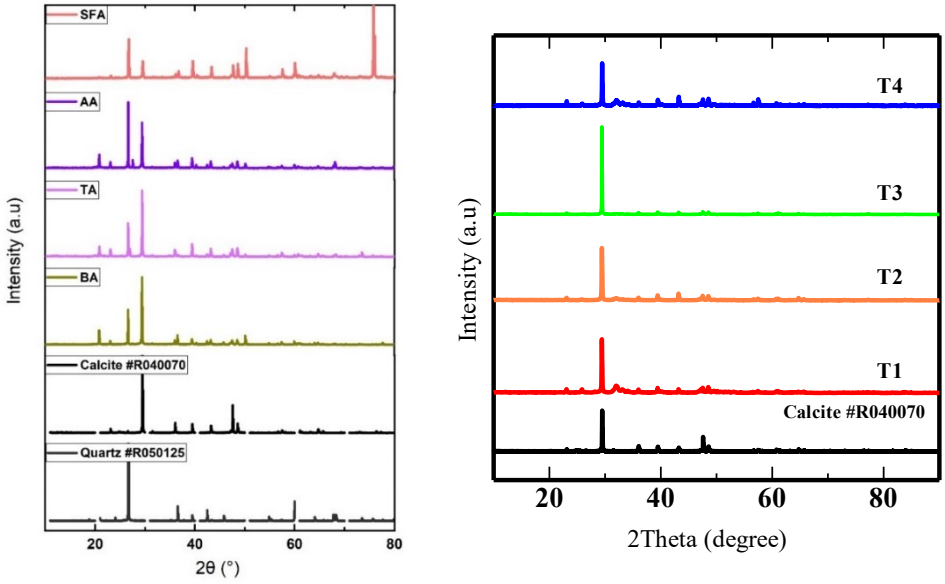

Figure 9 Minerals are dominated by Calcite ($CaCO_3$) R040070 and Quartz (SiO_2) R050125.

The minerals found during the analysis of the XRD data were found to be dominant, namely Calcite and Quartz. The most dominant calcite mineral found in fossil samples because the fossil itself consists of the elements Carbon (C) and Calcium (Ca) as constituents of the mineral Calcite. Meanwhile, in the sediment samples, we used other minerals, namely quartz. Quartz is the easiest common mineral to find in nature [50]. Quartz is composed of the element Silica which bonds with oxygen, with compounds (SiO_2). The nature of quartz itself is light and very easy to separate.

The chemical elements that form calcite crystals consist of calcium (Ca) and carbonate (CO_3). The crystal system of calcite is hexagonal with rhombohedral cleavage, colorless and transparent. Calcite has a specific gravity of 2.7 with a hardness of 3. Calcite can be gained from fine to coarse and can form as stalactites, oolithic, or pisolitic. Pure calcite is generally white, whereas impure (due to substitution) is gray, red, green, yellow, or brown. The element Calcium (Ca) in calcite can be replaced by metal elements as impurities which in a certain weight percentage form other mineral. Based on the physical properties of the crystal system, calcite can be distinguished from aragonite ($CaCO_3$). Compare with some study which be held; (1) The mineral from brantas river from Indonesia found dominated by magnetite (Fe_3O_4) [51]; (2) The study from Tallo tributary in Makasar City from Indonesia found that some mineral are Hematite (α-Fe_2O_3), Ilmenite ($FeTiO_3$), Goethite (α-FeOOH), Pyrrhotites (Fe_{1-xS}), Jacobsite ($MnFe_2O_4$), and Chromite ($FeCr_2O_4$) [52]; (3) The study from Ganges-Brahmaputra-Meghna river in Bangladesh. They found dominated by Illite $K_{0.65}Al_{2.0}[Al_{0.65}Si_{3.35}O_{10}](OH)_2$ [53].

Vibrating sample magnetometer (VSM)

VSM were carried out to see the magnetic properties in the sample. All samples are included in Diamagnetic properties. This property occurs because it does not contain a very strong magnetic material. So that the hysteresis curve that occurs does not change significantly in all samples. Can be seen in **Figures 10** and **11** confirm that the magnetic domain.

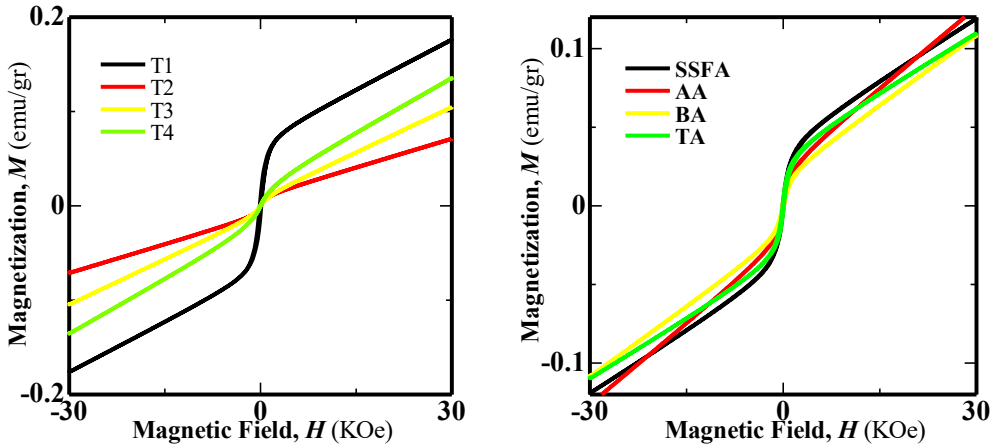

Figure 10 Hysteresis curve resulting from several samples. a) Samples with the Fossil Category, b) Sample category of pure sediments and sediments attached to fossils.

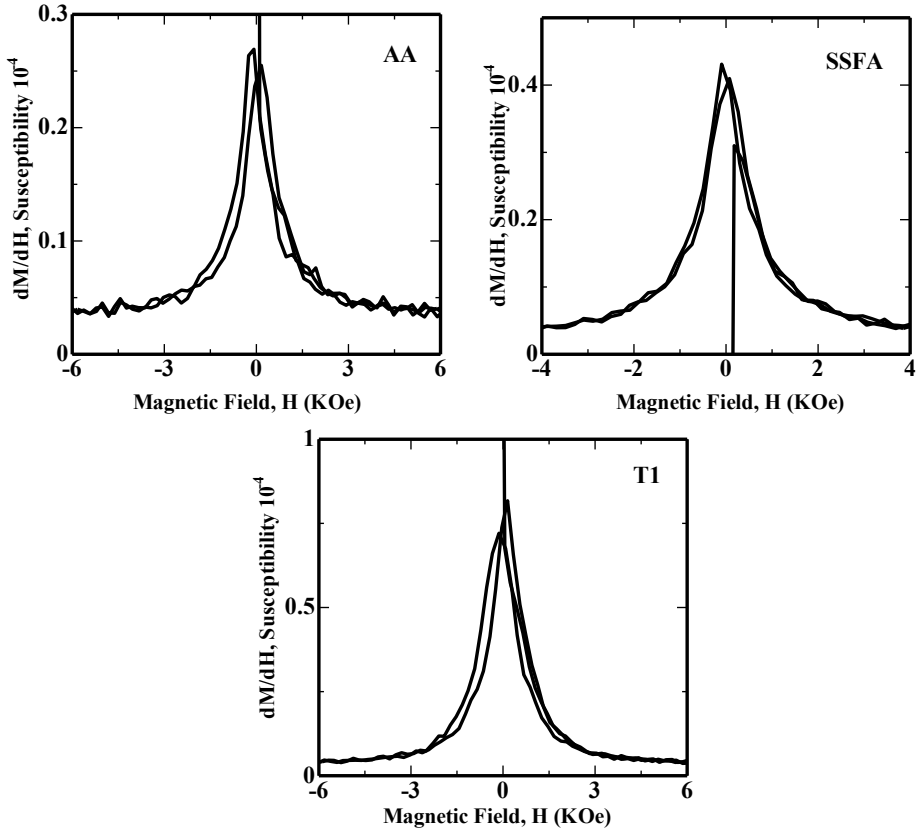

Figure 11 Magnetic domain representative of the 3 types of sample categories obtained.

In determining the magnetic domain of a material, it can be seen from the curve obtained from the results of the plot between magnetic susceptibility and the magnetic field of a material. By using the equation $\chi = dM/dH$ we get the magnetic domain curve. Of all the tests performed, we only display a few curves that are representative of the 3 sample categories. We get from all samples that belong to the multi-domain type. Based on the Mr/Ms value below 0.5, all of them show multi-domain results [54-57]. Magnetic remanent around 0.0001 - 0.004 emu/gr, while magnetic saturation around 0.071 - 0.176 emu/gr, and Magnetic Coercivity about 10.969 - 115.278 Oe.

Table 3 The value of Magnetic Remanent (Mr), Magnetic Saturation (Ms) dan Nilai Coercivity Field (Hc).

Code	Mr (emu/g)	Ms (emu/g)	Mr/Ms	Hc (Oe)
AA	0.003	0.126	0.024	122.628
TA	0.004	0.110	0.036	102.912
BA	0.002	0.108	0.019	110.185
SSFA	0.002	0.119	0.017	44.674
T1	0.009	0.176	0.051	115.278
T2	0.0002	0.071	0.003	46.089
T3	0.0001	0.105	0.0009	10.969
T4	0.0003	0.135	0.002	24.980
[46]*	Founded Ms ~ 0.9 *M/Ms* (Not mention of standard units)			
[51]*	They declare it Ms 5 - 6 Am^2Kg^{-1}			
[58]*	They found Ms 35.75 emu/gr			

*Another result from other area

Scanning electron microscope energy dispersion spectroscopy (SEM-EDS)

In determining the elements contained in the sample can use Energy dispersion spectroscopy (EDS) by showing the surface morphology of the sample. The results obtained can be seen in **Figure 12** confirms the surface shape of the sediment samples. The average grain size is 1.23 µm. The morphology that is clearly visible is that it is a spherical shape that is not symmetrical. Has a sharp angle caused by the erosion process that occurs in the sample. Erosion which is possible due to the factor of flooding or heavy water currents that occur for a long time. On the surface of the sample visible fine grains indicating that the process of mineral formation is incomplete. So that the cavity is filled by other elements. Thus, it will affect the yield of minerals contained in the sample. In **Table 4** it is divided into 3 observation points, namely point 1 to point 3. Each point produces a different element content. There is even an element that is only found at point 2 but is not found at points 1 and 3, namely the element Potassium (K). The element Potassium belongs to the alkane elements of the earth.

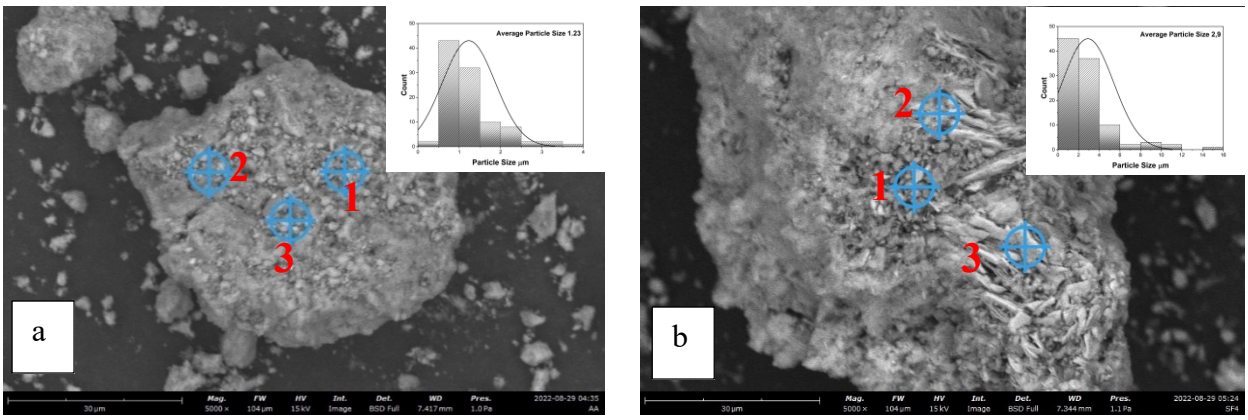

Figure 12 Morphology of a) sediment code AA, b) Fossil code T4.

Table 4 a) Element content point 1, b) point 2, and c) point 3.

Element symbol	Element name	Atomic conc.
	a	
C	Carbon	21.358
O	Oxygen	38.413
Al	Aluminium	0.848
Si	Silicon	2.351
Ca	Calcium	31.556
Fe	Iron	5.275
In	Indium	0.199
	b	
C	Carbon	11.829
O	Oxygen	33.160
Al	Aluminium	2.257
Si	Silicon	4.954
K	Potassium	1.038
Ca	Calcium	39.857
Fe	Iron	6.904
	c	
C	Carbon	12.713
O	Oxygen	39.194
Al	Aluminium	1.415
Si	Silicon	3.300
Ca	Calcium	38.300
Fe	Iron	5.077
[50]*	Al, Ca, Si, K, Ti, and Fe	
[53]*	As, Ba, Cd, Co, Cr, Cu, Hg, Mn, Mo, Ni, Pb, Sn, V, and Zn	

*Compare with another study

In **Figure 13** is the morphology of the fossil sample with point 4. It looks very different compared to **Figure 12**. This is caused by different types of samples and different minerals contained in the samples. In **Figure 12** there is a Quartz mineral which is very easy to find in the environment. Meanwhile, in **Figure 13** is a pure sample obtained from fossils. The most found mineral is Calcite ($CaCO_3$) and there is no Quartz mineral in it. Fossil surface forms that have cavities and a rough texture. Coarse texture caused by sampling that is not smooth. So that the texture of the fossil is still carried over. The most dominant element is O. At 3 points it produces different element concentrations. At point one the elements O, Mn and Ca predominate. The most abundant point found is carbon (C) with a concentration of 9.104 and 2.9 μm of average particle size.

At the second and third test points the most dominant elements were O, Mn, and F but had different concentrations from each other. At the second point the concentration of Mn decreased, and the concentration of F increased from the second point to the third point. This means that the Mn element accumulates the most at the second point, while Carbon (C) accumulates the most at the first point. Elemental Fluorine (F) accumulates the most at point one.

In the fossil samples, Fe was not found as a magnetic material contributor. So, it was confirmed that the results obtained in the Vibrating Sample Magnetometer test were correct. The curve obtained is almost straight.

Table 5 a) Element content point 1, b) point 2, and c) point 3.

Element symbol	Element name	Atomic conc.
	a	
C	Carbon	9.104
O	Oxygen	63.596
F	Fluorine	2.349
Si	Silicon	0.159
P	Phosphorus	1.369
Ca	Calcium	18.428
Mn	Manganese	4.996
	b	
C	Carbon	4.242
O	Oxygen	65.113
F	Fluorine	6.837
Mg	Magnesium	0.314
Ca	Calcium	1.907
Mn	Manganese	20.956
Ba	Barium	0.630
	c	
C	Carbon	3.248
O	Oxygen	63.534
F	Fluorine	13.215
Mg	Magnesium	0.501
Ca	Calcium	1.399
Mn	Manganese	17.216
Ba	Barium	0.887
[59]*	They found P, S, Cl, K, Ca, Ti, Mn, Fe, Ni, Cu and Zn	
[60]*	They declare S, P, Ca and Sr, Th, Y and Ce	
[61]*	They declare found Zn, As, Pb, Mn	

*Compare with another study

Conclusions

Identification of the morphology and magnetics present in sediment and fossil samples showed that the value of magnetic susceptibility or the value of the magnetic susceptibility of a material to receive an external magnetic field varied among the 3 sample categories obtained. The first type is pure sediment between 15.9×10^{-8} - 22.1×10^{-8} m^3/Kg; the second type is the sediment on the surface of the fossil, namely 37.8×10^{-8} m^3/Kg; and the third type is pure fossil powder ranging from 1.3×10^{-8} - 1.5×10^{-8} m^3/Kg. The results of magnetic susceptibility vary depending on the magnetic elements contained in the sample. It is proven that there are not many magnetic elements in the fossils or even the bones. Determination of magnetic minerals using X-Ray Diffractometer confirmed that Calcite ($CaCO_3$) and Quartz (SiO_2) predominate in the sample. Due to the predominance of non-magnetic minerals, the resulting hysteresis

curve is almost straight-line in shape. So, the magnetic properties of the sample are included in paramagnetic which will lead to diamagnetic properties. Thus, the morphology of the sediment is like an imperfect circle. This is due to the process of erosion by river water that lasts a long time and minerals that are not perfectly formed. The fossil samples on the surface are rough and stringy. Coarse fibers are characteristic of being formed from bones or fossils. So that the elements contained are also different from each other. In sediments the most dominant elements are C, O, Ca, Fe. There are still magnetic mineral elements, namely Fe, while the most dominant elemental fossil samples are C, O, Ca, Mn. There is no Fe element as a constituent of magnetic material in fossils.

Acknowledgements

This study was financially supported by Penelitian Dasar Unggulan Perguruan Tinggi (PDUPT) Universitas Sebelas Maret Surakarta Indonesia, contract number: 673.1/UN27.22/PT.01.03/2022.

References

[1] R Ono and A Pawlik. *Introductory chapter: Pleistocene archaeology - migration, technology, and adaptation*. Pleistocene Archaeology. IntechOpen, London, 2020.

[2] S Oliveira, K Nägele, S Carlhoff, I Pugach, T Koesbardiati, A Hübner, M Meyer, AA Oktaviana, M Takenaka, C Katagiri, DB Murti, RS Putri, Mahirta, F Petchey, T Higham, CFW Higham, S O'Connor, S Hawkins, R Kinaston, P Bellwood, ..., M Stoneking. Ancient genomes from the last three millennia support multiple human dispersals into Wallacea. *Nat. Ecol. Evol.* 2022; **6**, 1024-34.

[3] MR Fauzi, FS Intan and AS Wibowo. Newly discovered cave art sites from Bukit Bulan, Sumatra: Aligning prehistoric symbolic behavior in Indonesian prehistory. *J. Archaeol. Sci. Rep.* 2019; **24**, 166-74.

[4] S Sumarjono, K Swastika, M Na'im, AR Pratama and RN Jamil. Historical interpretation: Traces of classic culture in Situbondo, East Java. *Budapest Int. Res. Critics Inst. J.* 2022; **5**, 205-7.

[5] HC Hung, Hartatik, TA Ma'rifat and T Simanjuntak. Mongol fleet on the way to Java: First archaeological remains from the Karimata Strait in Indonesia. *Archaeol. Res. Asia* 2022; **29**, 100327.

[6] HAF Kaharudin, GAR Ananda, WH Prasetya, MW Wibisono and JSE Yuwono. Hunter-gatherers in labyrinth karst: An Early Holocene record from Gunung Sewu, Java. *Archaeol. Res. Asia* 2023; **33**, 100427.

[7] Y Rizal, KE Westaway, Y Zaim, GDVD Bergh, EA Bettis, MJ Morwood, OF Huffman, R Grün, R Joannes-Boyau, RM Bailey, Sidarto, MC Westaway, I Kurniawan, MW Moore, M Storey, F Aziz, Suminto, Z Jian-Xin, Aswan, ME Sipola, ..., RL Ciochon. Last appearance of Homo erectus at Ngandong, Java, 117,000-108,000 years ago. *Nature* 2020; **577**, 381-5.

[8] KL Baab, M Rogers, E Bruner and S Semaw. Reconstruction and analysis of the DAN5/P1 and BSN12/P1 Gona Early Pleistocene Homo fossils. *J. Hum. Evol.* 2022; **162**, 103102.

[9] SL Hilgen, E Pop, S Adhityatama, TA Veldkamp, HWK Berghuis, I Sutisna, D Yurnaldi, G Dupont-Nivet , T Reimann, N Nowaczyk, KF Kuiper, W Krijgsman, HB Vonhof, DR Ekowati, G Alink, NLGDM Hafsari, O Drespriputra, A Verpoorte, R Bos, ..., JCA Joordens. Revised age and stratigraphy of the classic *Homo erectus*-bearing succession at Trinil (Java, Indonesia). *Quaternary Sci. Rev.* 2023; **301**, 107908.

[10] S Matsu'ura, M Kondo, T Danhara, S Sakata, H Iwano, T Hirata, I Kurniawan, E Setiyabudi, Y Takeshita, M Hyodo, I Kitaba, M Sudo, Y Danhara and F Aziz. Age control of the first appearance datum for Javanese Homo erectus in the Sangiran area. *Science* 2020; **367**, 210-4.

[11] HWK Berghuis, A Veldkamp, S Adhityatama, SL Hilgen, I Sutisna, DH Barianto, EAL Pop, T Reimann, D Yurnaldi, DR Ekowati, HB Vonhof, T Kolfschoten, T Simanjuntak, JM Schoorl and JCA Joordens. Hominin homelands of East Java: Revised stratigraphy and landscape reconstructions for Plio-Pleistocene Trinil. *Quaternary Sci. Rev.* 2021; **260**, 106912.

[12] HWK Berghuis, T Kolfschoten, S Adhityatama, SR Troelstra, S Noerwidi, RA Suriyanto, UP Wibowo, E Pop, I Kurniawan, SL Hilgen, A Veldkamp and JCA Joordens. The eastern Kendeng Hills (Java, Indonesia) and the hominin-bearing beds of Mojokerto, a re-interpretation. *Quaternary Sci. Rev.* 2022; **295**, 107692.

[13] S Subanti, I Slamet, W Sulandari, E Zukhronah, S Sugiyanto and I Susanto. Profile of tourist visits in Sangiran Site Area, Sragen Regency. *J. Math. Math. Educ.* 2021; **11**, 21-31.

[14] S Noerwidi, A Vialet, H Widianto, I Kurniawan, J Zaim, RA Suriyanto, J Joordens, C Lorenzo, T Simanjuntak and F Sémah. Exploring the diversity of fossil hominin dental patterns in the western Indonesian archipelago during the Quaternary by Geometric Morphometric Analysis. Application on

second upper and lower molars. *L'Anthropologie* 2020; **124**, 102791.
[15] Rihayati, S Utaminingsih and Santoso. Improving critical thinking ability through discovery learning model based on patiayam site ethnoscience. *J. Phys. Conf.* 2021; **1823**, 012104.
[16] M Shulton. Redesigning the patiayam kudus archaeological museum with a regionalism architecture approach muhammad. *Nat. Sci. Eng. Tech. J.* 2022; **1**, 18-23.
[17] F Sémah, AM Sémah, T Simanjuntak and Widianto. *Humans in Island Southeast Asia Prior to Homo sapiens Settlement, with Special Reference to Java Island*. Oxford Handbooks, Oxford, England, 2022.
[18] AAEVD Geer, GA Lyras and R Volmer. Insular dwarfism in canids on Java (Indonesia) and its implication for the environment of *Homo erectus* during the Early and earliest Middle Pleistocene. *Palaeogeography Palaeoclimatology Palaeoecology* 2018; **507**, 168-79.
[19] C Zanolli, O Kullmer, J Kelley, AM Bacon, F Demeter, J Dumoncel, L Fiorenza, FE Grine, JJ Hublin, AT Nguyen, TMH Nguyen, L Pan, B Schillinger, F Schrenk, MM Skinner, X Ji and R Macchiarelli. Evidence for increased hominid diversity in the Early to Middle Pleistocene of Indonesia. *Nat. Ecol. Evol.* 2019; **3**, 755-64.
[20] K Weber, DE Winkler, ES Kornas, TM Kaiser and T Tütken. Post-mortem enamel surface texture alteration during taphonomic processes - Do experimental approaches reflect natural phenomena? *PeerJ* 2022; **10**, e12635.
[21] G Herrera-Franco, N Montalván-Burbano, P Carrión-Mero, B Apolo-Masache and M Jaya-Montalvo. Evidence of unknown paleo-tsunami events along the Alas Strait, West Sumbawa, Indonesia. *Geosciences* 2020; **10**, 379.
[22] C Gomez, Y Shinohara, H Tsunetaka, N Hotta, B Bradak and Y Sakai. Twenty-five years of geomorphological evolution in the gokurakudani gully (Unzen volcano): Topography, subsurface geophysics and sediment analysis. *Geosciences* 2021; **11**, 457.
[23] JB Winarto, WA Nurlathifah, A Djafar, AD Sipayung, RAP Sari and H Insani. The surficial basin sediment investigation and its concerned vertebrate fossils in Sirtwo Island, Western Part of Saguling Dam, West Java, Indonesia. *Indonesian J. Earth Sci.* 2022; **2**, 1-15.
[24] PWM Souza-Filho, TC Giannini, R Jaffé, AM Giulietti, DC Santos, WRN Jr, JTF Guimarães, MF Costa, VL Imperatriz-Fonseca and JO Siqueira. Mapping and quantification of ferruginous outcrop savannas in the Brazilian Amazon: A challenge for biodiversity conservation. *PLos One* 2019; **14**, e0211095.
[25] J Wakabayashi. Sedimentary compared to tectonically-deformed serpentinites and tectonic serpentinite mélanges at outcrop to petrographic scales: Unambiguous and disputed examples from California. *Gondwana Res.* 2019; **74**, 51-67.
[26] R Booysen, S Lorenz, ST Thiele, WC Fuchsloch, T Marais, PAM Nex and R Gloaguen. Accurate hyperspectral imaging of mineralised outcrops: An example from lithium-bearing pegmatites at Uis, Namibia. *Rem. Sens. Environ.* 2022; **269**, 112790.
[27] P Palermo, MA Irurzun, CSG Gogorza, AM Sinito, C Ohlendorf and B Zolitschka. Rock-magnetic and paleomagnetic studies on late-Holocene sediments from Laguna Cháltel (Patagonia, Argentina). *J. S. Am. Earth Sci.* 2019; **90**, 204-15.
[28] P Jaqueto, RIF Trindade, F Terra-Nova, JM Feinberg, VF Novello, NM Stríkis, P Schroedl, V Azevedo, BE Strauss, FW Cruz, H Cheng and RL Edwards. Stalagmite paleomagnetic record of a quiet mid-to-late Holocene field activity in central South America. *Nat. Comm.* 2022; **13**, 1349.
[29] P Zhao, E Appel, B Xu and T Sukhbaatar. First paleomagnetic result from the early permian volcanic rocks in Northeastern mongolia: Evolutional implication for the Paleo-Asian ocean and the mongol-okhotsk ocean. *J. Geophys. Res. Solid Earth* 2020; **125**, e2019JB017338.
[30] ZI Levitt. *Paleomagnetic constraints on assembly of the superior craton: Results from the 2.72-2.69 Ga Vermilion District of the Wawa Subprovince, MN*. Massachusetts Institute of Technology, Massachusetts, 2022.
[31] H Oda, W Katanoda, A Usui and M Murayama. Rotation of a ferromanganese nodule in the Penrhyn Basin, South Pacific, tracked by the earth's magnetic field. *G-cubed* 2023; **24**, e2022GC010789.
[32] DG Schulze. *An introduction to soil mineralogy*. *In*: JB Dixon and DG Schulze (Eds.). Soil Mineralogy with Environmental Applications. John Wiley & Sons.
[33] B González-Grijalva, D Meza-Figueroa, FM Romero, A Robles-Morúa, M Meza-Montenegro, L García-Rico and R Ochoa-Contreras. The role of soil mineralogy on oral bioaccessibility of lead: Implications for land use and risk assessment. *Sci. Total Environ.* 2019; **657**, 1468-79.
[34] BEB Nurhandoko, R Kurniadi, Susilowati , K Triyoso, S Widowati, MR Hadi, MR Abda, RK Martha, E Fatiah and IR Komara. Integrated subsurface temperature modeling beneath Mt. Lawu and Mt.

Muriah in The Northeast Java Basin, Indonesia. *Open Geosci.* 2019; **11**, 341-51.
[35] AMB Jones. *Early Tenth Century Java from the Inscriptions*. Brill, Leiden, Netherlands, 1984.
[36] L Zhang, Q Zhao, S Peng, Z Qiu, C Feng, Q Zhang, Y Wang, D Dong and S Zhou. Paleoenvironment and organic matter accumulation mechanism of marine-continental transitional shales: Outcrop characterizations of the carboniferous-permian strata, ordos basin, North China. *Energies* 2021; **14**, 7445.
[37] N Chien and Z Wan. *Mechanics of sediment transport*. American Society of Civil Engineers, Washington DC, 1999.
[38] CB Zhou, YF Chen, R Hu and Z Yang. Groundwater flow through fractured rocks and seepage control in geotechnical engineering: Theories and practices. *J. Rock Mech. Geotech. Eng.* 2023; **15**, 1-36.
[39] LP Fearman and JC Ellison. Lithological controls influence river form in contrasting sub-catchments: The Scamander and Avenue Rivers, Tasmania. *River Res. Appl.* 2023; **39**, 861-74.
[40] S Mulyaningsih, S Bronto, A Kusniadi, L Apriyanti, L Budiyanto and DA Wiloso. The Petrology and Volcano-Stratigraphy of The Muria-Peninsula High-K Volcanic Rocks, Central Java, Indonesia. *J. Geosci. Eng. Environ. Tech.* 2022; **7**, 69-80.
[41] N Peez, J Becker, SM Ehlers, M Fritz, CB Fischer, JHE Koop, C Winkelmann and W Imhof. Quantitative analysis of PET microplastics in environmental model samples using quantitative 1H-NMR spectroscopy: Validation of an optimized and consistent sample clean-up method. *Anal. Bioanalytical Chem.* 2019; **411**, 7603.
[42] JC Prata, IF Sequeira, SS Monteiro, ALP Silva, JPD Costa, P Dias-Pereira, AJS Fernandes, FMD Costa, AC Duarte and T Rocha-Santos. Preparation of biological samples for microplastic identification by Nile Red. *Sci. Total Environ.* 2021; **783**, 147065.
[43] D Urbancl, D Goricanec and M Simonic. Zero-waste approach for heavy metals' removal from water with an enhanced multi-stage hybrid treatment system. *Materials* 2023; **16**, 1816.
[44] M Elkelawy, HAE Bastawissi, KK Esmaeil, AM Radwan, H Panchal, KK Sadasivuni, D Ponnamma and R Walvekar. Experimental studies on the biodiesel production parameters optimization of sunflower and soybean oil mixture and DI engine combustion, performance, and emission analysis fueled with diesel/biodiesel blends. *Fuel* 2019; **255**, 115791.
[45] J Yang, M Monnot, Y Sun, L Asia, P Wong-Wah-Chung, P Doumenq and P Moulin. Microplastics in different water samples (seawater, freshwater, and wastewater): Methodology approach for characterization using micro-FTIR spectroscopy. *Water Res.* 2023; **232**, 119673.
[46] M Li, S Zhu, T Ouyang, J Tang and Z Tang. Magnetic properties of the surface sediments in the Yellow River Estuary and Laizhou Bay, Bohai Sea, China: Implications for monitoring heavy metals. *J. Hazard. Mater.* 2021; **410**, 124579.
[47] JF Li, EJ Rupa, J Hurh, Y Huo, L Chen, Y Han, JC Ahn, JK Park, HA Lee, R Mathiyalagan and DC Yang. Cordyceps militaris fungus mediated zinc oxide nanoparticles for the photocatalytic degradation of methylene blue dye. *Optik* 2019; **183**, 691-7.
[48] KS Rodygin, YA Vikenteva and VP Ananikov. Calcium-based sustainable chemical technologies for total carbon recycling. *ChemSusChem* 2019; **12**, 1483-516.
[49] N Gussone, ASC Ahm, KV Lau and HJ Bradbury. Calcium isotopes in deep time: Potential and limitations. *Chem. Geol.* 2020; **544**, 119601.
[50] B Legowo, S Putra, H Purwanto, H Rifai, W Suryanto and B Purnama. Magnetic properties of ancient sediments bengawan solo , central Java-East Java, Indonesia. *Trends Sci.* 2023; **20**, 6626.
[51] M Mariyanto, MF Amir, W Utama, AM Hamdan, S Bijaksana, A Pratama, R Yunginger and S Sudarningsih. Heavy metal contents and magnetic properties of surface sediments in volcanic and tropical environment from Brantas River, Jawa Timur Province, Indonesia. *Sci. Total Environ.* 2019; **675**, 632-41.
[52] VA Tiwow, Subaer, Sulistiawaty, JD Malago, MJ Rampe and M Lapa. Magnetic susceptibility of surface sediment in the Tallo tributary of Makassar city. *J. Phys. Conf.* 2021; **1899**, 012124.
[53] GN Salomão, R Dall'Agnol, PK Sahoo, RS Angélica, CADM Filho, JDSF Júnior, MSD Silva, PWMS Filho, WDRN Junior, MFD Costa, LRG Guilherme and JOD Siqueira. Geochemical mapping in stream sediments of the Carajás Mineral Province: Background values for the Itacaiúnas River watershed, Brazil. *Appl. Geochem.* 2020; **118**, 104608.
[54] N Boda, G Boda, KCB Naidu, M Srinivas, KM Batoo, D Ravinder and AP Reddy. Effect of rare earth elements on low temperature magnetic properties of Ni and Co-ferrite nanoparticles. *J. Magn. Magn. Mater.* 2019; **473**, 228-35.
[55] N Raghuram, TS Rao and KCB Naidu. Magnetic properties of hydrothermally synthesized $Ba_{1-x}Sr_xFe_{12}O_{19}$ (x = 0.0–0.8) nanomaterials. *Appl. Phys. Mater. Sci. Process.* 2019; **125**, 839.

[56] A Gaffoor, KCB Naidu, D Ravinder, KM Batoo, SF Adil and M Khan. Synthesis of nano-$NiXFe_2O_4$ (X = Mg/Co) by citrate-gel method: Structural, morphological and low-temperature magnetic properties. *Appl. Phys. Mater. Sci. Process.* 2020; **126**, 39.

[57] TV Sagar, TS Rao and KCB Naidu. Effect of calcination temperature on optical, magnetic and dielectric properties of Sol-Gel synthesized $Ni_{0.2}Mg_{0.8-x}Zn_xFe_2O_4$ (x = 0.0–0.8). *Ceram. Int.* 2020; **46**, 11515-29.

[58] B Legowo, B Julica, Suharyana, AT Wijayanta and B Purnama. Local distribution of the hematite content in a fine sediments of Bengawan Solo river. *AIP Conf. Proc.* 2018; **2014**, 020122.

[59] V Rossi, SM Webb and ME McNamara. Hierarchical biota-level and taxonomic controls on the chemistry of fossil melanosomes revealed using synchrotron x-ray fluorescence. *Sci. Rep.* 2020; **10**, 8970.

[60] J Li, R Pei and X Xu. Micro-XRF study of the troodontid dinosaur Jianianhualong tengi reveals new biological and taphonomical signals. *Atom. Spectros.* 2021; **41**, 1-11.

[61] P Gueriau, S Réguer, N Leclercq, C Cupello, PM Brito, C Jauvion, S Morel, S Charbonnier, D Thiaudière and C Mocuta. Visualizing mineralization processes and fossil anatomy using synchronous synchrotron x-ray fluorescence and x-ray diffraction mapping. *J. R. Soc. Interface* 2020; **17**, 20200216.